Int j simul model 19 (2020) 2, 231-242
ISSN 1726-4529 Original scientific paper

MECHANICAL PERFORMANCES ANALYSIS OF TENSION-TORSION COUPLING ANCHOR CABLE

Wang, S. R.[*,**,#]; Wang, Z. L.[**]; Chen, Y. B.[**]; Wang, Y. H.[**] & Huang, Q. X.[*,***]
[*] International Joint Research Laboratory of Henan Province for Underground Space Development and Disaster Prevention, Henan Polytechnic University, Jiaozuo 454003, China
[**] School of Civil Engineering, Henan Polytechnic University, Jiaozuo 454003, China
[***] College of Energy Engineering, Xi'an University of Science and Technology, Xi'an 710054, China
E-Mail: w_sr88@163.com ([#] Corresponding author)

Abstract
To reveal the tension-torsion coupling effect of the anchor cable, the three-dimension computational model was built. The mechanical performances of the anchor cable under tension-torsion coupling were studied by the analytical analysis and simulation verification on the model, and the coupling coefficient of the tension-torsion was proposed to define the percentage of the tensile force used for untwisting. The axial stress, shear stress and plastic development of the cross-section of the anchor cable were analysed also. Results show that the influence of the torsion of the anchor cable on the tensile force cannot be ignored. The tension-torsion coupling coefficient and the torque both increase with the increase of the diameter and the lay angle of the anchor cable. The maximum equivalent stress of the cross-section of the pulling anchor cable appears in the contact area of the inner and outer wires, and is larger under the free rotation than that under the restricted rotation condition. With the increase of the lay angle, the elastic modulus and the bearing capacity of the anchor cable decrease. The obtained conclusions can provide a reference for the similar practice of the anchor cable.
(Received in February 2020, accepted in May 2020. This paper was with the authors 1 month for 1 revision.)

Key Words: Anchor Cable, Simulation Modelling, Tension-Torsion, Equivalent Stress, Rotation

1. INTRODUCTION

The anchor cable is a kind of steel strand which is composed of several high-strength steel wires around the central straight steel wire. Because of the high bearing capacity, active support, good toughness and other characteristics, the anchor cable has been widely used in a large number of slope, tunnel and mining engineering practices in the world [1, 2].

Although there are lots of research on the mechanical properties of the steel strands [3-5]. But most scholars focus on the mechanical properties of the anchor cable under the restricted rotation condition. In practical engineering, due to the influence of the spiral structure and anchorage interface, the anchor cable will produce a torque perpendicular to the section when it is pulled. This torque will make the strands of the anchor cable rotate reversely, thus reducing the axial force of the anchor cable. There are few reported studies on the tensile mechanical properties of the anchor cable under the free rotation condition, and the relevant mechanism of the tension-torsion coupled effects is not clear.

Therefore, it is of important theoretical significance and practical value to study the mechanical performance and the tension-torsion coupling characteristics of the steel strand under the conditions of free and restricted rotation, which can be used for the failure prediction, structural design optimization of the anchor cable.

2. STATE OF THE ART

Since the structure of the single strand wire rope is similar to the steel strand, the corresponding research results can be used for the reference. Kang et al. found that the displacement in the elastic range of the steel strand was very small and which tended to

increase with the increase of the diameter of the steel strand [6]. Xing et al. analysed the influence of different strain rates on the mechanical properties of the prestressed steel strand [7]. Utting and Jones carried out the tensile tests on the fixed and free-load ends of the single strand wire ropes with different lay angles [8].

The analytical method has gradually developed for the accuracy and low cost. Hruska proposed a simple analytical model for predicting the tensile properties of the single strand wire rope, but he ignored the bending and torsional stiffness of the single wire [9]. Considering the torsional stiffness of the steel wire, McConnell and Zemke pointed out that the tension and torsion of the steel wire were coupled with each other based on the Hruska model [10]. Based on Love's curved bar theory, Machida and Durelli studied the influence of the bending and torsional stiffness of the single steel wire on the stiffness matrix of the whole rope [11]. Costello put forward a nonlinear analytical model to predict the mechanical properties of the single strand wire rope [12]. Kumar and Cochran linearized Costello's equation and they derived the linearization and closed expression of the axial stiffness coefficient [13]. Argatov established an analytical model of the steel wire rope by simplifying the contact between the central and the spiral steel wire [14]. Foti and Martinelli established an elastic-plastic analytical model of the single strand wire rope under tension and torsion, but they ignored the Poisson's ratio effect [15].

The finite element method can not only reflect the geometric and stress conditions of the steel strand, but also consider many nonlinear factors that are difficult to be considered by the analytical method. Ghoreishi et al. evaluated the effectiveness and limitations of various linear static analysis models of the steel strand under the tensile load [16]. Yu et al. studied the mechanical properties and stress state among the strands under the transverse load [17]. Chen et al. analysed the contact stress of the simple round rope strand and the spiral triangle strand under the axial tension and torsion under the restricted rotation [18]. There do still exist the following problems: the research on anchor cables is mainly pure tensile mechanical properties, and its torsional properties are ignored. The tensile and torsional coupling effects are not explained from the perspective of microscopic stress. In addition, due to the differences in materials and structures of the steel wire ropes and strands, there is few reports on systematic optimization of the tensile properties of the steel strands under the free and restricted rotations.

Taking three kinds of diameter anchor cables commonly used in mine engineering as the samples, through theoretical analysis and numerical simulation, the tensile performances and the coupling characteristics of the anchor cables were studied under the free rotation and restricted rotations. The remainder of this study is organized as follows: Section 3 introduces the mechanical and numerical modelling process of the anchor cable under the restricted and free rotations. Section 4 analyses and discusses the tensile performance and the tension-torsion coupling effects of the anchor cable. Section 5 summarizes the conclusions drawn from this study.

3. METHODOLOGY

3.1 Mechanical analysis of anchor cable

The structure of the steel strand is shown in Fig. 1 a. The structural parameters of the steel strand mainly include the lay length, lay angle and helix radius. The lay length is the length of the steel strand corresponding to the outer wire rotating one circle around the inner wire. The lay angle is the angle between the tangent of the outer wire and the inner wire. The helix angle and the lay angle are complementary to each other. The helix radius is equal to the sum of the inner and outer wire radius. When the steel strand is under tension, it will produce a torque, which will cause the anchor cable to rotate reversely if it is not restrained.

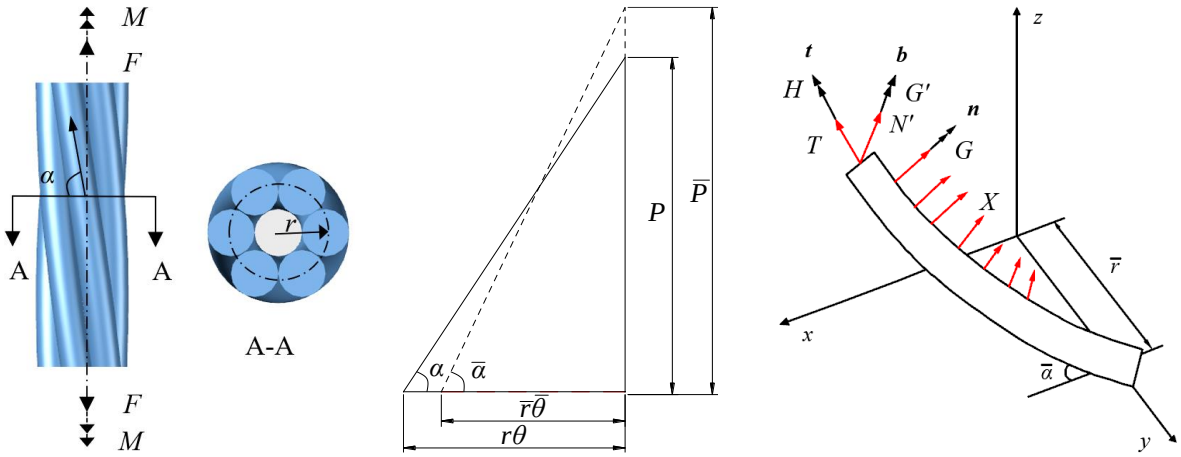

Figure 1: Mechanical modelling of steel strand: a) Structural of steel strand; b) Central line expansion of spiral steel wire; c) Forces and moments of spiral steel wire.

Select one lay length optionally, and unfold the outer wire around the inner wire is shown in Fig. 1 b. In the initial state, the structural parameters meet the following relationship:

$$P = 2\pi r \tan\alpha \tag{1}$$

where, P is the lay length; α is the helix angle; r is the helix radius; θ is the angle of rotation around the centre wire when the outer wire is twisted, when the spiral steel wire is twisted for one circle, $\theta = 2\pi$, which is a lay length. The twist shape of the spiral steel wire will change under the axial load of the steel strand. After deformation, the axial strain and the rotation angle of the unit length of the steel strand can be expressed as [12]:

$$\varepsilon = \frac{\bar{P}\text{-}P}{P} = \varepsilon_0 = (1+\varepsilon_1)\frac{\sin\bar{\alpha}}{\sin\alpha}\text{-}1 \tag{2}$$

$$\theta_z = \frac{\bar{\theta}-\theta}{P} = \frac{1+\varepsilon_0}{\bar{r}\tan\bar{\alpha}} - \frac{1}{r\tan\alpha} \tag{3}$$

where, ε is the steel strand axial strain; ε_0 is the inner wire axial strain, obviously $\varepsilon = \varepsilon_0$; ε_1 is the outer wire axial strain; $\bar{P}$, $\bar{\alpha}$, $\bar{r}$ are the lay length, helix angle and helix radius of the steel strand after deformation, respectively. θ_Z is the rotation angle of the unit length of the steel strand. Assuming that the inner and outer wire radius are equal to R, Poisson's ratio is v, and ignoring the contact deformation among the steel wires, the spiral radius after loading changes to:

$$\bar{r} = R(1\text{-}\nu\varepsilon_0) + R(1\text{-}\nu\varepsilon_1) = r - \nu R(\varepsilon_0 + \varepsilon_1) \tag{4}$$

Based on the theory of Love's curved bar, the forces and moments diagram of the spiral steel wire is shown in Fig. 1 c, where T and H are the axial force and torque of the steel wire on the tangent ***t*** direction, respectively; N' and G' are the shear force and bending moment on the subnormal ***b*** direction, respectively; X and G are the unit line contact force and the bending moment in the normal ***n*** direction, respectively. The corresponding calculation formulas can be found in [12].

According to the section projection relationship, the axial tension and torque acting on the steel strand are:

$$F = \pi R^2 E\varepsilon_0 + 6\left(T\sin\bar{\alpha} + N'\cos\bar{\alpha}\right) \tag{5}$$

$$M = M_0 + 6\left(H\sin\bar{\alpha} + G'\cos\bar{\alpha} + T\bar{r}\cos\bar{\alpha} - N\bar{r}\sin\bar{\alpha}\right) \tag{6}$$

where, M_0 is the torque of the inner wire, $M_0 = \frac{\pi E R^4}{4(1+\nu)}\theta_z$ and it is zero without rotation, E is the elastic modulus of the steel wire.

Eqs. (5) and (6) can be converted into:

$$\begin{vmatrix} F \\ M \end{vmatrix} = \begin{bmatrix} k_{11} & k_{12} \\ k_{21} & k_{22} \end{bmatrix} \begin{vmatrix} \varepsilon \\ \theta_z \end{vmatrix} \tag{7}$$

where, k_{11}, k_{22}, k_{12} and k_{21} are the tensile and torsional stiffness, tensile-torsional stiffness and torsional-tensile stiffness of the steel strand, respectively. Kumar and Cochran have linearized Costello's model to obtain the corresponding four stiffness component expressions [13]. Therefore, the stiffness component of the steel wire can be calculated by programming and substitute it into the following formulas to analysis the tensile mechanical properties of the steel strand.

When the steel strand is under the restricted rotation, according to $\theta_z = 0$,

$$\varepsilon = \frac{F}{k_{11}}, \qquad M = \frac{k_{21}}{k_{11}} F \tag{8}$$

When the steel strand is under the free rotation, according to $M = 0$,

$$\varepsilon = \frac{F k_{22}}{k_{11}k_{22} - k_{12}k_{21}} \tag{9}$$

3.2 Numerical analysis of anchor cable

Computational model and calculation parameters: The three-dimension model of the steel strand is established by ABAQUS [19, 20]. The length of the model is taken as a lay length, and the structural parameters of three different diameter steel strands are listed in Table I based on the actual measurement.

Table I: Structural parameters of steel strand.

Strand diameter (mm)	**Internal wire diameter** (mm)	**Outside wire diameter** (mm)	**Lay angle** (°)	**The length of model** (mm)
9.5	3.26	3.12	7.63	150
12.7	4.34	4.18	7.63	200
15.2	5.20	5.00	8.70	210

The 8-node reduced integral facade element C3D8R is used to mesh the steel strand by the method of scanning. To accurately show the stress distribution of the section, especially the contact area, the mesh size should be fine enough, but too small element size will increase the computer burden. After the grid convergence analysis, the radial and axial direction of the single steel wire are taken as 17 and 140 units to balance the calculation accuracy and efficiency, respectively. The mesh division of the model is shown in Fig. 2.

The material parameters of steel strand are measured according to the tensile test of steel wire. It should be noted that the plastic parameters in ABAQUS require the true stress-strain of the input material, so the nominal stress-strain curve measured in the experiment needs to be transformed. The constitutive parameters after transformation are shown in Table II.

Boundary conditions and loading methods: The contact between the adjacent wires is calculated by the general contact adaptive contact algorithm. The normal direction of the contact surface is hard contact, the tangential contact is calculated by the penalty function method, and the friction coefficient is 0.1. The freedom degrees of the nodes on the end faces

of each wire at both ends of the anchor cable are coupled with the reference points respectively by means of motion coupling. The fixed end constrains all degrees of freedom; the loading end only opens the axial displacement degrees of freedom under the restricted rotation and opens the axial displacement and rotation degrees of freedom under the free rotation. Due to the strong nonlinearity of the steel strand, the static algorithm is difficult to converge, so the ABAQUS/Explicit simulation quasi-static method is used to simulate the mechanical characteristics of the anchor cable. By displacement loading, the tensile distance is 6.2 % of the model length.

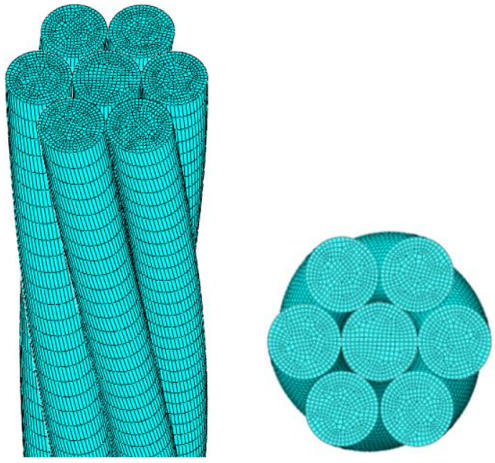

a) b)

Figure 2: Computational model and its meshes of cable-bolts: a) Computational model; b) Cross-section of the model.

Table II: Material parameters of steel strand.

Elastic modulus (GPa)	**Poisson's ratio**	**Density** (t/m^3)	**Yield strength** (MPa)	**Tensile strength** (MPa)	**Plastic train**
210	0.30	7.85	1810	2020	0.05

4. RESULTS AND DISCUSSION

4.1 Mechanical performances of pulling anchor cable

The comparison between the simulation and the analytical results under the conditions of restricted and free rotation of three kinds of diameter anchor cables are shown in Fig. 3. It can be seen from Fig. 3, the simulation results are in good agreement with the analytical results in the elastic stage, which verifies the accuracy of the mechanical model. In addition, the elastic modulus of the anchor cable decreases and the trend of the plastic phase is slower under the condition of free rotation. While the tensile force in the plastic phase increases faster than that under the restricted rotation. The tension and torque of the anchor cable are linear in the elastic stage under the restricted rotation, and the torque increases with the increase of the anchor cable diameter.

To evaluate the influence degree of the torsion on the tensile force of the anchor cable, according to the functional principle, it can be known that under the free rotation, part of the work done by the tensile force is used to untwist ignoring the friction and other factors. The work induced by the rotation of the anchor cable is equivalent to that of the reverse rotation force ΔF in the tensile displacement. Therefore, the coupling coefficient of the tension and torsion is proposed to define the percentage of the tensile force used for the untwisting of the anchor cable.

$$\eta = \frac{\Delta F}{F} = \frac{2(W_1 - W_2)}{FS} \tag{10}$$

where, η is the tension-torsion coupling coefficient; ΔF is the reverse rotation force, kN; F is the tensile force, kN; W_1 is the work done under the restricted condition, W_2 is the work done under the free rotation condition, which can be obtained by integrating the axial force-deformation curve, J; S is the strain of the anchor cable.

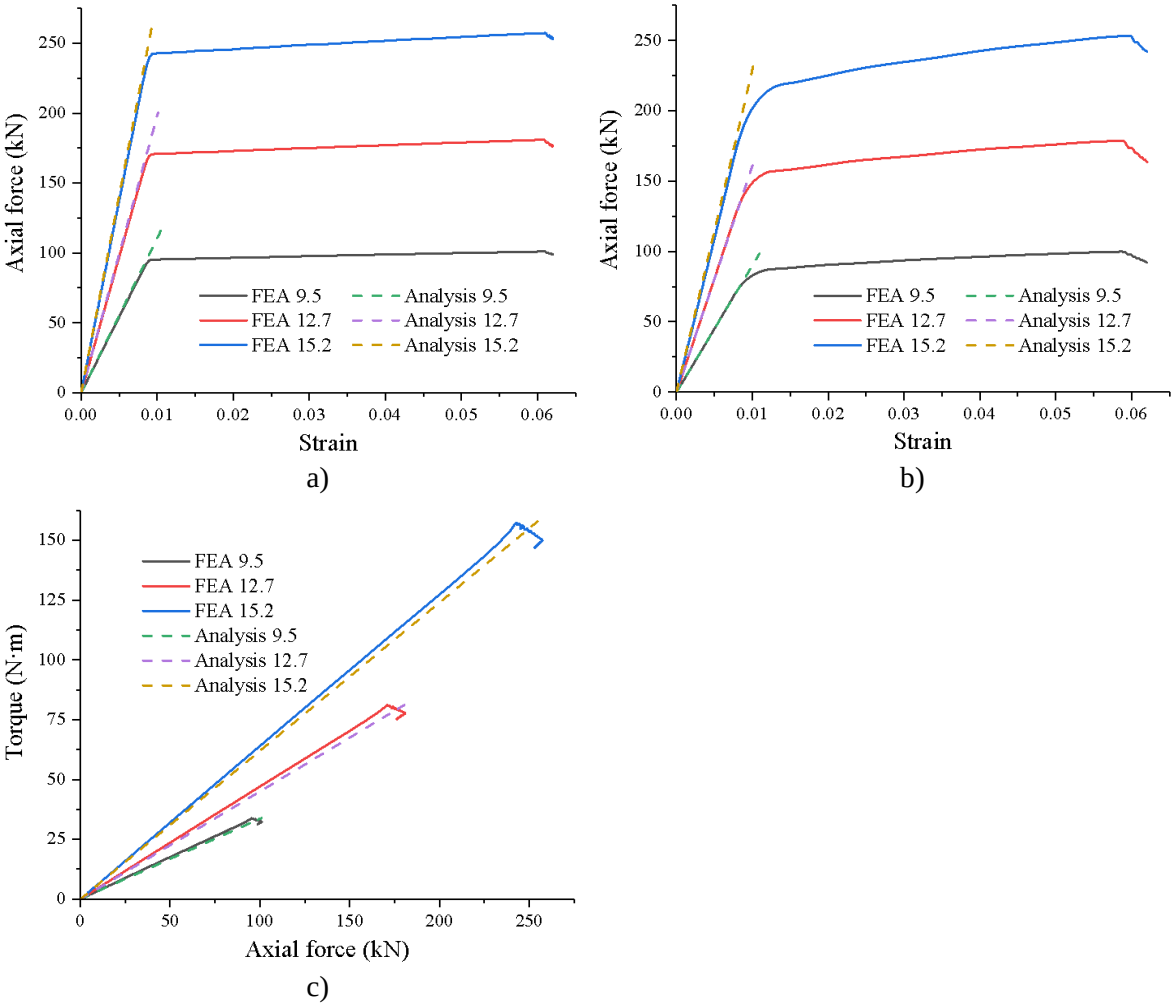

Figure 3: Axial force-strain and torque-axial force curves under different conditions: a) Under restricted rotation; b) Under free rotation; c) Under restricted rotation.

According to Figs. 3 a and 3 b, the coupling coefficients of the tension-torsion of three kinds of diameter anchor cables are 10 %, 12 % and 14 %, respectively. It can be seen that the influence of the torsion of the anchor cable on the tensile force cannot be ignored, and the coupling coefficients of the tension and torsion increase with the increase of the anchor cable diameter.

4.2 Equivalent stress analysis of anchor cable

It is adopted the equivalent stress to analyse the comprehensive stress state of the anchor cable. Due to the stress distributions of the three kinds of the diameters are similar, the 15.2 mm cable was regarded as the example to analyse the tension-torsion coupling characteristics. When the strain in the elastic phase is 0.64 %, the section equivalent stress distribution of the anchor cable under the conditions of restricted and free rotations are shown in Fig. 4.

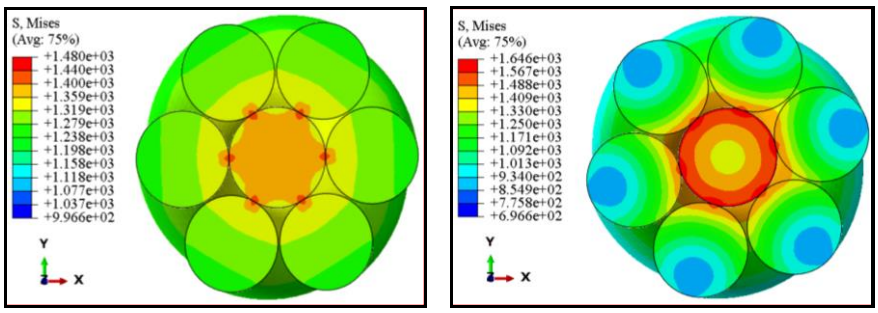

a) b)

Figure 4: Equivalent stress of 15.2 mm diameter anchor cable under two conditions (MPa): a) Restricted rotation; b) Free rotation.

As seen from Fig. 4, in the case of the restricted rotation, the equivalent stress at the place where the internal and external steel wires contact is larger, followed by the central steel wire and the outer steel wire of the anchor cable is the smallest. Due to the existence of the contact pressure, the local stress concentration occurs in the inner and outer contact areas, but it has little effect on the overall distribution. The stress distribution of the central steel wire is relatively uniform, and the outer steel wire decreases in layers from the inside to the outside of the anchor cable. Under the condition of the free rotation, it is also the place where the internal and external steel wires contact of the anchor cable is the largest, due to the influence of the torsion, there is a certain range of the stress concentration in the contact areas of the internal and external wires. Starting from the contact area, the central steel wire decreases from the outside to the inside in a concentric circle form, but the outer steel wire decreases from the inside to the outside in a half moon form, showing obvious delamination.

It can be seen from Fig. 5, there is no obvious difference among these anchor cables under the same boundary conditions. The equivalent stress is greater in the free rotation case than in the restricted rotation case, which indicates that the torsion intensifies the stress concentration of the anchor cable. The anchor cable is easy to yield under the torsion stress, and the torsion stress is an unfavourable loading mode. The order of the equivalent stress of three kinds of the diameters in different conditions is 9.5 mm < 12.7 mm < 15.2 mm, it shows that with the increase of the diameter, the stress concentration degree of the anchor cable increases, but the increase is not obvious.

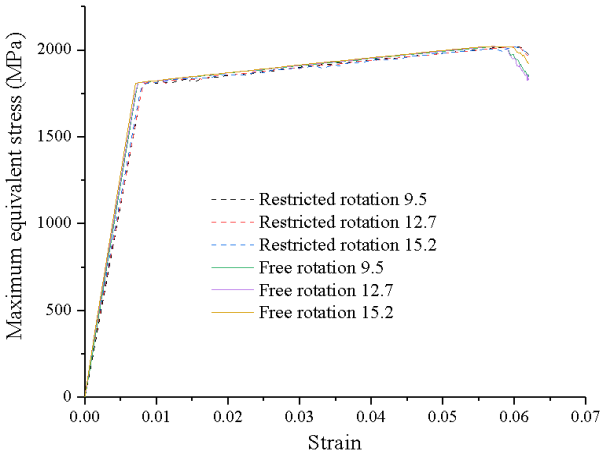

Figure 5: The maximum equivalent stress-strain curves of different cable diameters.

4.3 Tension-torsion coupling effects of anchor cable

Axial stress: When the strain is 0.64 %, the axial stress of the cross-section of the anchor cable under the conditions of the restricted and free rotations is shown in Fig. 6. It can be seen

from Fig. 8, the axial stress distribution of the anchor cable is relatively uniform without rotation, and the place where the inner and outer wires contact is smaller, because the place is not only pulled but also squeezed. Among these wires, the axial stress of the inner wire is the largest, and the outer wire decreases gradually from the inside to the outside, with a little change. Under the condition of the free rotation, the axial stress distribution is extremely uneven. The axial stress of the inner wire is larger, which of the outer wire is gradually reduced from the inside to the outside, the layering phenomenon is obvious.

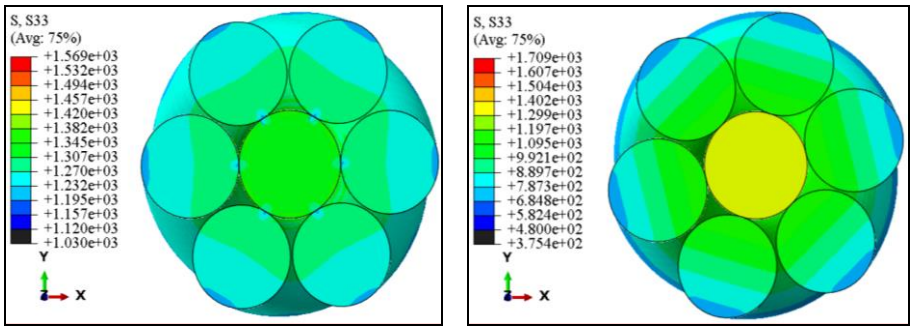

a) b)

Figure 6: The cross-section axial stresses under two conditions: a) Restricted rotation; b) Free rotation.

As can be seen from Fig. 7, the mean value of the axial stress of the cross-section under free rotation is smaller than that under the restricted rotation, therefore, the provided tensile force under the same elongation is smaller, and the elastic modulus is reduced. On the other hand, the elastic modulus of the steel strand will be reduced because part of the external work done by the axial load is used to untwist in the case of free rotation.

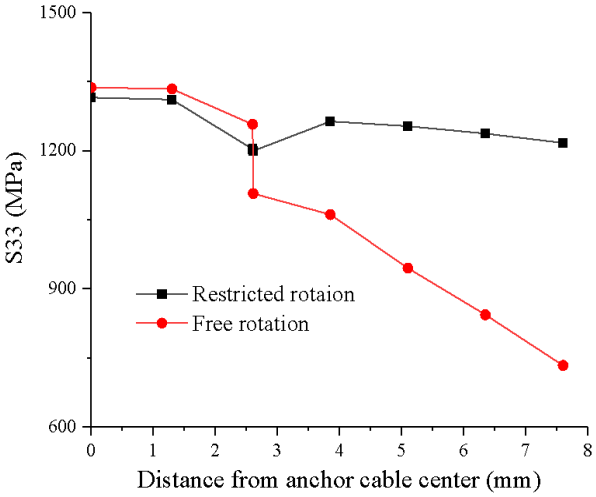

Figure 7: The axial stress distribution curves of anchor cable.

Shear stress: As can be seen from Fig. 8, the shear stress of the inner wire under the restricted rotation condition is positive (untwisting direction) and approximately zero, indicating that it does not twist. The shear stress of the outer steel wire is negative (tight rotation direction), because it is restrained by the counter torque. In the case of the free rotation, the cross-section shear stress distribution is in a petal form, and the value of the contact area of the inner and outer wires is close and the direction is opposite, which indicates that the inner wire is also twisted by the shear effect of the outer wire, and the internal and external torque cancel each other. The central wire decreases in concentric circles from the outside to the inside, and the shear stress in the external wire gradually changes from negative to positive, and there is a critical layer in the middle of the anchor cable.

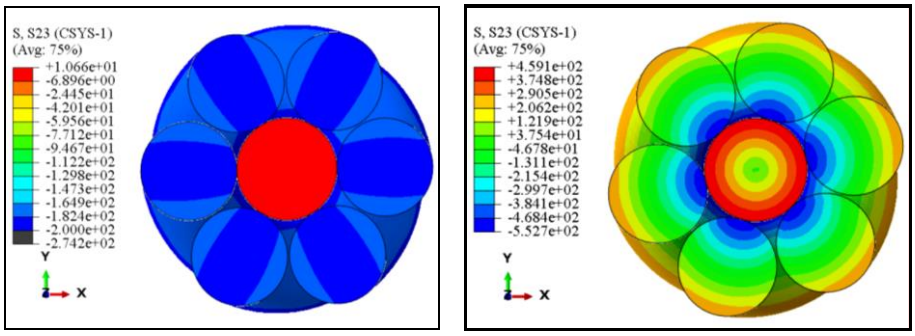

a) b)

Figure 8: The cross-section shear stress under two conditions: a) Restricted rotation; b) Free rotation.

The shear stress values at different positions from the centre of the anchor cable are extracted as shown in Fig. 9. It can be found from Fig. 9 that the shear stress is distributed uniformly under the restricted rotation, and the shear stress fluctuates greatly under the free rotation condition.

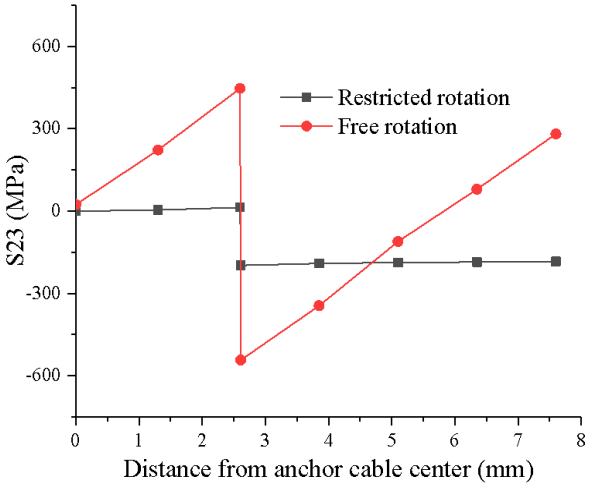

Figure 9: Shear stress distribution curves of anchor cable.

Elastoplastic state: As seen from Fig. 10, the points on the cross-section of the anchor cable reach the yield stress almost simultaneously under the restricted rotation condition, which makes the elastic-plastic transition stage on the tension-strain curve change sharply.

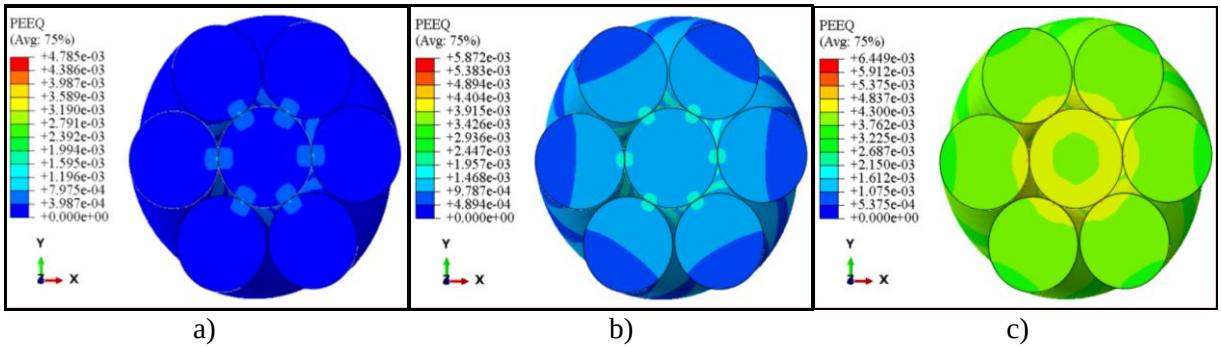

a) b) c)

Figure 10: Equivalent plastic strain evolution with different strains under restricted rotation: a) 0.93 %; b) 1.09 %; c) 1.27 %.

As can be seen from Fig. 11, in the case of the free rotation, the plastic flow starts from the highest point of the equivalent stress and gradually spreads on the steel wire cross-section of the anchor cable, resulting in a slow transition from the elastic stage to the plastic stage.

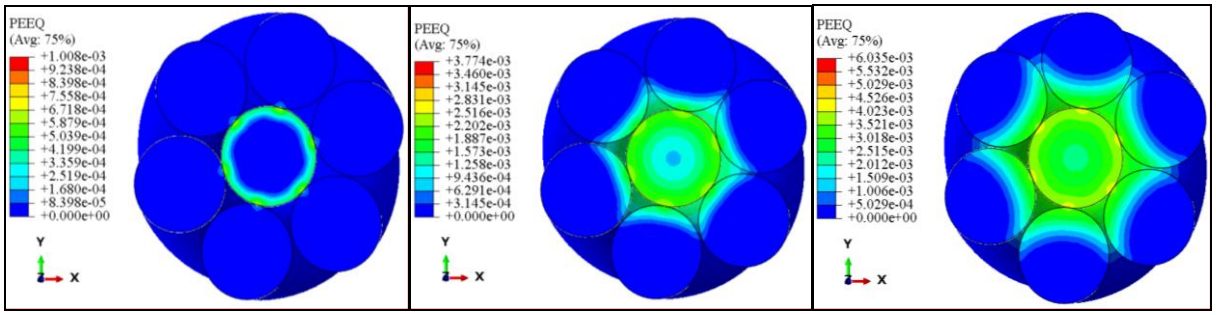

a) b) c)

Figure 11: Equivalent plastic strain evolution with different strains under free rotation; a) 0.78 %; b) 0.93 %; c) 1.09 %.

4.4 Lay angle effect on pulling steel strand

The lay angle is an important geometric parameter of the anchor cable, which greatly affects on the mechanical properties of the anchor cable. According to China's GB5224-2014 specification, the lay length of 1860 MPa steel strands with a diameter of 15.24 mm should be 12-16 times of the diameter, and the corresponding lay angle is 7.52 °-9.98 °, so three kinds of the finite element models of the steel strand with different lay angles of 6 °, 8 °, and 10 ° are established, respectively. Taking the lay length as the model length, and the material parameters are the same as listed in Table II.

As seen from Fig. 12 a, when the anchor cable is not rotating, the elastic modulus and bearing capacity decrease slightly with the increase of the twist angle. With the lay angle increasing, the helicity of the steel wire increases and the contact stress increases. As can be seen from Fig. 12 b, with the increase of the lay angle, the elastic modulus and bearing capacity of the steel strand are reduced under the free rotation. But the degree of decline is more obvious than that under the restricted rotation, indicating that the response to the change of the lay angle is more sensitive under the free rotation.

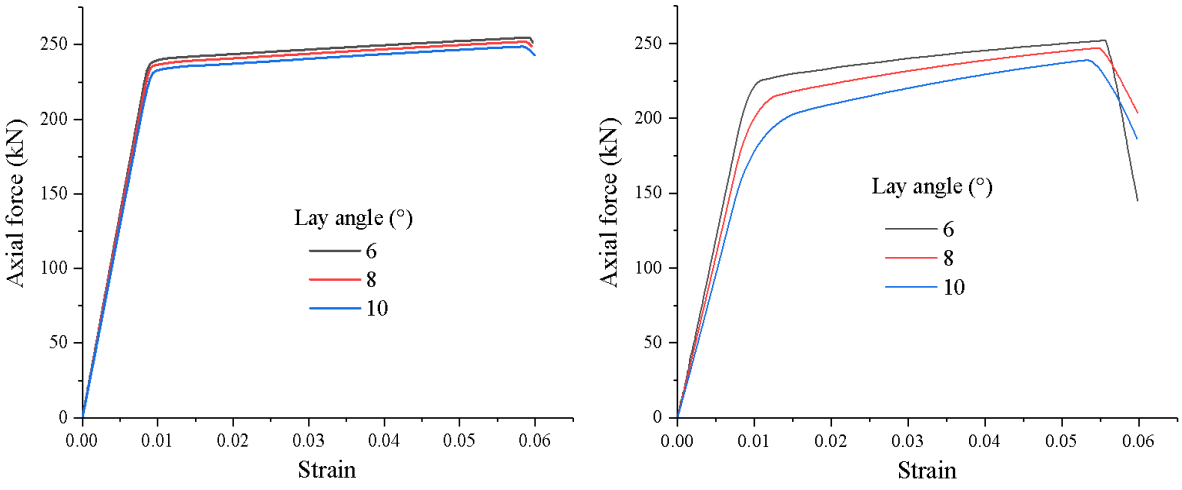

a) b)

Figure12: Axial force-strain curves under different conditions: a) Under restricted rotation; b) Under free rotation.

As can be seen from Fig. 13, with increase of the lay angle, the torque of the steel strand also increases. According to Eq. (10), the tension-torsion coupling coefficients of the three lay angle cables can be obtained 6.1 %, 11.6 % and 19.3 %, respectively, which indicates the larger the twist angle is, the more serious the tensile force loss of the steel strand caused by the rotation. Therefore, the strength of the steel strand can be improved by reducing the lay

angle. However, if the twist angle is too small, it will lead to the increase of the elastic stress and the deterioration of the softness of the wire rope.

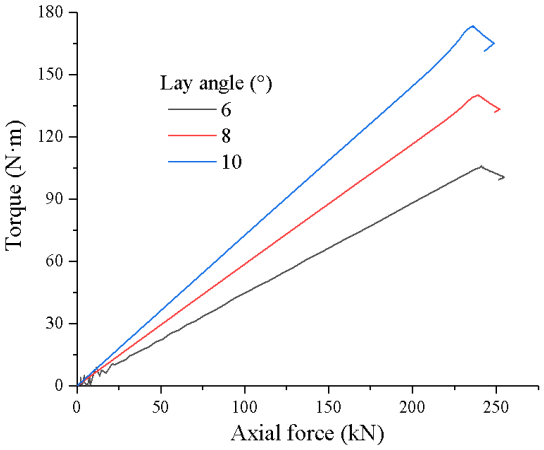

Figure13: Torque-tension curve with different lay angles under restricted rotation.

Moreover, the default lay angle of the steel strand in the production process cannot be less than 7°. When the twist angle is less than 7°, the twisted steel wire does not undergo the plastic mapping, and the steel wire cannot maintain the spiral shape, which makes the stranded wire extremely easy to loose and the wire has a large elastic stress. Therefore, when choosing the lay angle of the steel strand, it is necessary to consider all kinds of factors, and then make a reasonable choice.

5. CONCLUSIONS

Taking three kinds of diameter anchor cables as samples, the mechanical properties and tension-torsion coupling effects of the anchor cables under free and restricted rotations were studied, and the main conclusions are as follows.

The coupling coefficient of the tension-torsion and the torque both increase with the increase of the diameter and lay angle of the anchor cable. The maximum equivalent stress appears in the contact area of the internal and external wires, and the equivalent stress is large when it is under the free rotation. The torsion aggravates the uneven degree of the stress of the outer wire, causing the decrease of the mean value of the axial stress of the section under the same strain. With the increase of the lay angle, the elastic modulus and the ultimate bearing capacity of the steel strand are decreasing. Choosing the lay angle of the steel strand is necessary to consider all kinds of factors and then make a reasonable choice.

The conclusions can provide a reference for the evaluation of the pulling anchor cable under the free and restricted rotations. However, the anchor cable not only bears the tensile and torsional loads, but also shear, bending, impact and other loads, so the mechanical properties of the anchor cable can be further studied under the complex loads.

ACKNOWLEDGEMENT

This work was supported by the National Natural Science Foundation of China (51774112), the Doctoral Fund of Henan Polytechnic University in China (B2015-67).

REFERENCES

[1] Jolicoeur, C.; Cardou, A. (1991). A numerical comparison of current mathematical models of twisted wire cables under axisymmetric loads, *Journal of Energy Resources Technology*, Vol. 113, No. 4, 241-249, doi:10.1115/1.2905907

[2] Huo, B. J.; Jin, X. D.; Cao, C. (2019). Anchorage mechanical characteristics of newly designed rebar bolt and optimization of its support scheme, *Journal of Engineering Science and Technology Review*, Vol. 12, No. 2, 93-97, doi:10.25103/jestr.122.13
[3] Wang, S. W.; Feng, J. L.; Jia, X. R.; Yao, X. F. (2000). Comparison study on wire rope models, *Mechanics in Engineering*, Vol. 22, No. 5, 8-13, doi:10.3969/j.issn.1000-0879.2000.05.002
[4] Cheng, L.-K. (2005). Research and new progress in ground anchorage, *Chinese Journal of Rock Mechanics and Engineering*, Vol. 24, No. 21, 3803-3811
[5] Wang, S. R.; Xiao, H. G.; Hagan, P.; Zou, Z. S. (2017). Mechanical behavior of fully-grouted bolt in jointed rocks subjected to double shear tests, *DYNA*, Vol. 92, No. 3, 314-320, doi:10.6036/8325
[6] Kang, H. P.; Yang, J. H.; Jiang, P. F. (2015). Tests and analysis on mechanical properties for cable bolts, *Coal Science and Technology*, Vol. 43, No. 6, 29-33, doi:10.13199/j.cnki.cst.2015.06.006
[7] Xing, X. K.; Li, Y.; Lei, Z. L.; Li, Q. (2018). Dynamic mechanical tensile properties and constitutive relationship of prestressed steel strand, *Science Technology and Engineering*, Vol. 18, No. 7, 228-233, doi:10.3969/j.issn.1671-1815.2018.07.041
[8] Utting, W. S.; Jones, N. (1987). The response of wire rope strands to axial tensile loads – Part II. Comparison of experimental results and theoretical predictions, *International Journal of Mechanical Sciences*, Vol. 29, No. 9, 621-636, doi:10.1016/0020-7403(87)90034-8
[9] Hruska, F. H. (1951). Calculation of stresses in wire ropes, *Wire and Wire Products*, Vol. 26, No. 9, 766-767
[10] McConnell, K. G.; Zemke, W. P. (1982). A model to predict the coupled axial torsion properties of ACSR electrical conductors, *Experimental Mechanics*, Vol. 22, No. 7, 237-244, doi:10.1007/BF02326388
[11] Machida, S.; Durelli, A. J. (1973). Response of a strand to axial and torsional displacements, *Journal of Mechanical Engineering Science*, Vol. 15, No. 4, 241-251, doi:10.1243/JMES_JOUR_1973_015_045_02
[12] Costello, G. A. (1992). *Theory of wire rope*, book, Bert, C. W. (Reviewer), *Journal of Applied Mechanics*, Vol. 59, No. 2, 469, doi:10.1115/1.2899552
[13] Kumar, K.; Cochran, Jr., J. E. (1987). Closed-form analysis for elastic deformations of multilayered strands, *Journal of Applied Mechanics*, Vol. 54, No. 4, 898-903, doi:10.1115/1.3173136
[14] Argatov, I. (2011). Response of a wire rope strand to axial and torsional loads: Asymptotic modeling of the effect of interwire contact deformations, *International Journal of Solids and Structures*, Vol. 48, No. 10, 1413-1423, doi:10.1016/j.ijsolstr.2011.01.021
[15] Foti, F.; Martinelli, L. (2016). Mechanical modeling of metallic strands subjected to tension, torsion and bending, *International Journal of Solids and Structures*, Vol. 91, 1-17, doi:10.1016/j.ijsolstr.2016.04.034
[16] Ghoreishi, S. R.; Messager, T.; Cartraud, P.; Davies, P. (2007). Validity and limitations of linear analytical models for steel wire strands under axial loading, using a 3D FE model, *International Journal of Mechanical Sciences*, Vol. 49, No. 11, 1251-1261, doi:10.1016/j.ijmecsci.2007.03.014
[17] Yu, Y. J.; Chen, Z. H.; Liu, H. B.; Wang, X. D. (2014). Finite element study of behavior and interface force conditions of seven-wire strand under axial and lateral loading, *Construction and Building Materials*, Vol. 66, 10-18, doi:10.1016/j.conbuildmat.2014.05.009
[18] Chen, Y. P.; Meng, F. M.; Gong, X. S. (2015). Parametric modeling and comparative finite element analysis of spiral triangular strand and simple straight strand, *Advances in Engineering Software*, Vol. 90, 63-75, doi:10.1016/j.advengsoft.2015.06.011
[19] Billenstein, D.; Dinkel, C.; Rieg, F. (2018). Automated topological clustering of design proposals in structural optimisation, *International Journal of Simulation Modelling*, Vol. 17, No. 4, 657-666, doi:10.2507/IJSIMM17(4)454
[20] Cheng, L. Z.; Liu, D. K.; Wang, Y.; Chen, A. Q. (2019). Load distribution and contact of axle box bearings in electric multiple units, *International Journal of Simulation Modelling*, Vol. 18, No. 2, 290-301, doi:10.2507/IJSIMM18(2)475